PROCEEDINGS OF SCIENCE

The efficient low-mass Seyfert MCG–05–23–016

V. Beckmann*[ab], S. Soldi[ab], T.J.-L. Courvoisier[ab], N. Gehrels[c], P. Lubiński[ad], J. Malzac[e], P.O. Petrucci[f] and C. R. Shrader[c]

[a] *ISDC Data Centre for Astrophysics, 1290 Versoix, Switzerland*
[b] *Observatoire Astronomique de l'Université de Genève, 1290 Sauverny, Switzerland*
[c] *Astrophysics Science Division, NASA Goddard Space Flight Center, MD 20771, USA*
[d] *Centrum Astronomiczne im. M. Kopernika, PL-00-716 Warszawa, Poland*
[e] *Centre d'Étude Spatiale des Rayonnements, 31028 Toulouse Cedex 4, France*
[f] *Laboratoire d'Astrophysique de Grenoble, Univ. J. Fourier/CNRS, 38041 Grenoble, France*
E-mail: Volker.Beckmann@unige.ch

The Seyfert 1.9 galaxy MCG–05–23–016 has been shown to exhibit a complex X-ray spectrum. This source has moderate X-ray luminosity, hosts a comparably low-mass black hole, but accretes at a high Eddington rate, and allows us to study a super massive black hole in an early stage. Three observations of the INTEGRAL satellite simultaneous with pointed Swift/XRT observations performed from December 2006 to June 2007 are used in combination with public data from the INTEGRAL archive to study the variability of the hard X-ray components and to generate a high-quality spectrum from 1 to 150 keV. The AGN shows little variability in the hard X-ray spectrum, with some indication of a variation in the high-energy cut-off energy ranging from 50 keV to $\gg$ 100 keV, with an electron plasma temperature in the 10 - 90 keV range. The reflection component is not evident and, if present, the reflected fraction can be constrained to $R < 0.3$ for the combined data set. The AGN exhibits a remarkably high Eddington ratio of $L_{bol}/L_{Edd} > 0.8$ (or $L_{bol}/L_{Edd} > 0.1$, if we consider a higher mass of the central engine) and, at the same time, a low cut-off energy around 70 keV. Here we discuss in detail the mass estimate and its implications for our understanding of this Seyfert galaxy. Objects like MCG–05–23–016 might indicate the early stages of super massive black holes, in which a strong accretion flow feeds the central engine.

7th INTEGRAL Workshop
September 8-11 2008
Copenhagen, Denmark

*Speaker.

PoS(Integral08)058

1. Introduction

Active galactic nuclei (AGN) are commonly assumed to be super massive black holes in the centre of galaxies, in which accretion processes give rise to emission throughout the electromagnetic spectrum. AGN are observed to date up to redshifts of $z \sim 6.4$ [1], showing that super massive black holes with masses of $M_{BH} \sim 10^8\,\mathrm{M}_\odot$ must have been formed as early as < 0.7 Gyrs after the formation of the first stars [2]. In order to be able to form super massive black holes at this early stage of the Universe, merging events and high accretion rates are required. This black hole evolution is closely tied to the growth of the bulge of the AGN's host galaxy, as both seem to be correlated with $M_{BH} \simeq 10^{-3} M_{Bulge}$ [3].

Recent studies intend to not only find unification models for the different AGN types but also probe whether their central engines and super massive black holes are simply up-scaled versions of Galactic black holes like Cyg X–1, GRO J1655–40, or GX 339–4. In this context, models of black hole accretion can be tested using objects showing extreme physical properties, like luminosity, accretion rate, or Eddington ratio. The Seyfert 1.9 galaxy presented here resides in an extreme end of the known parameter space of AGN. X-ray observations give a direct view on matter close to the super massive black hole, providing insights into the geometry and the state of the matter. The flux and spectral variability of the sources in the hard X-rays reflect the size and physical state of the regions involved in the emission processes (see [4] for a brief review).

MCG–05–23–016 is one of the brightest Seyfert galaxies in the X-rays. This Seyfert 1.9 galaxy at redshift $z = 0.0085$ has not only been studied in the $2-10\,\mathrm{keV}$ band by most X-ray missions so far, but has also been detected in hard X-rays above 20 keV with *BeppoSAX*/PDS [5], *INTEGRAL*/IBIS [6], and *Swift*/BAT [7]. With a bolometric luminosity of $L_{bol} \simeq 2 \times 10^{44}\,\mathrm{erg\,s^{-1}}$ this Seyfert is a moderately luminous object, with a comparably small central black hole of $M_{BH} = 2 \times 10^6\,\mathrm{M}_\odot$ [8]. Wang & Zhang used the width of the OIII line [9] to obtain the black hole mass from the $M_{BH} - \sigma$ relation [10] and give the error of the measurement with 0.7 dex.

Recently, observations on MCG–05–23–016 by *Suzaku* showed a $0.4-100\,\mathrm{keV}$ spectrum which appeared to be a cut-off power law of $\Gamma = 1.9$ and $E_C > 170\,\mathrm{keV}$ plus a dual reflector with $R \sim 0.9$ and $R \sim 0.5$, respectively [11]. *XMM-Newton* and *Chandra* data confirmed that the iron Kα line complex consists of a broad and of a narrow component and revealed evidence for outflowing material [12]. The exact shape and structure of the high-energy spectrum of MCG–05–23–016 remains elusive though. *INTEGRAL* and *Swift* observations have been performed recently and the detailed analysis has been described in Beckmann et al. 2008 [13]. Here we discuss in more detail the mass estimate for the central engine and its implications for objects like MCG–05–23–016, with emphasis on similarities with Galactic black hole systems and on the fact that the Seyfert galaxy apparently operates at high Eddington ratio.

2. The hard X-ray emission

In our study of MCG–05–23–016 we have made use of the hard X-ray capabilities of *INTEGRAL*, and in particular of the imager IBIS/ISGRI, in combination with the soft X-ray spectrum provided by *Swift*/XRT. Although the combined spectrum does not provide the wealth of information in the soft X-rays as shown in *XMM-Newton*, *Chandra*, and *Suzaku* data, the better sensitivity

at energies above 30 keV puts significant constraints on the hard X-ray component. First of all, a high-energy cut-off in the range 57 keV to 86 keV is required in most of the observed *INTEGRAL* and *Swift* spectra. However, one observation in December 2006 shows a spectrum extending up to ~ 200 keV, excluding a cut-off at 50 keV on a 3σ level, and at 90 keV on a 1σ level, even when allowing for a different photon index of the underlying power law at the same time. It is important to note though, that the spectrum in this case is significantly steeper ($\Gamma = 1.7 \pm 0.1$) than in the cases where a cut-off is measured ($\Gamma = 1.5 \pm 0.1$).

The differences in the hard X-ray spectrum, i.e. the differences in high-energy cut-off and spectral slope, can be interpreted as different temperatures of the electron plasma, which is the source of the inverse Compton emission thought to be the dominant component in this energy range. The so called *compTT* model [14] for Comptonization of soft photons by a hot plasma includes the plasma temperature T_e of the hot corona, the optical depth τ_p of this plasma, and the temperature T_0 of the soft photon spectrum. Because the spectrum starts at $E \simeq 0.7$ keV, T_0 is not well constrained by the data and has been fixed to 10 eV.

As for the cut-off energy E_C, the variation of the plasma temperature is significant on a 2σ level. The highest plasma temperature and lowest optical depth are observed in December 2006, when the cut-off in the hard X-ray spectrum disappeared. However, it has to be taken into account that the December 2006 spectrum can also be fit by applying the same *compTT* model which gives the best fit to all data (i.e. with $kT_e = 18$ keV and $\tau_p = 2.5$) with an acceptable fit result ($\chi^2_\nu = 1.09$ for 52 d.o.f.). Similar values for cut-off energy and photon index as presented here were derived previously based on combined *BeppoSAX* and *INTEGRAL* IBIS/ISGRI data, resulting in $E_C = 112^{+40}_{-43}$ keV, $\Gamma = 1.74^{+0.08}_{-0.14}$, plus a reflection component with $R = 1.2^{+0.6}_{-1.0}$ [15]. As these observations are not simultaneous, these values have to be taken with some caution though, and the reflection component is not well constrained.

Apart from the variation of the cut-off energy and of the plasma temperature, describing a variable inverse Compton process, the low level of the reflection component in the data studied here is remarkable. The 2σ upper limit is $R < 0.25$, while in the observations presented by Reeves et al. (2007), a value of $R < 0.7$ can be excluded on a 3σ level. We have to conclude that the strong reflection component, visible in the December 2005 data taken by *Suzaku*, *XMM-Newton* and *Chandra* disappeared within a year. Also the excess observed at soft X-rays by Reeves et al. is only detectable in the *Swift*/XRT data of December 2005 and not afterwards. At the same time, also the iron line complex has decreased in flux, from an equivalent width of $EW = 130 \pm 17$ eV in December 2005 to about $EW = 61 \pm 45$ eV in 2006/2007. Unfortunately the *Swift*/XRT data do not allow us to disentangle the broad and narrow line components of the line complex, as reported in Balestra et al. (2004) and also in Reeves et al. (2007). If we assume that the narrow and the broad line components arise from two different absorbers with the broad line being emitted closer and the narrow line further away from the central engine as proposed by Reeves et al., then we might indeed observe the disappearance of the broad iron line ($EW \simeq 60$ eV [11]) and of the reflection component connected to the close absorber between the December 2005 and December 2006 observations, leaving the spectrum only with the narrow line component and reflection from the distant absorber. This disappearance is not accompanied by a significant change in X-ray luminosity or in UV/optical flux. The lack of hard X-ray flux variability appeared also in a study of MCG–05–23–016 using *Swift*/BAT, which resulted in a marginal variability of 6 ± 4% on a

20 day time scale [7]. The soft X-ray spectrum in the range 2–10 keV however appears to be variable by a factor of ~ 1.7 throughout historic observations. The *Swift*/XRT data presented here show a flux of $f_{2-10\,\mathrm{keV}} = (7.1-8.1)\times 10^{-11}\,\mathrm{erg\,cm^{-2}\,s^{-1}}$, with literature values in the range $f_{2-10\,\mathrm{keV}} = (7.1-11.9)\times 10^{-11}\,\mathrm{erg\,cm^{-2}\,s^{-1}}$ [16, 5].

A similar behaviour, of a hardening of the spectra with decreasing reflection component as we see it from comparison with previous measurements, has been observed before. Zdziarski, Lubinski & Smith (1999) analysed this relation for 61 *Ginga* observations of 24 radio quiet Seyfert galaxies. They found a strong correlation of the form $R = u\,\Gamma^{v}$ with the parameters $u = (1.4\pm 1.2)\,10^{-4}$ and $v = 12.4\pm 1.2$. The observed trend follows closely this relation. Our measurement of $\Gamma = 1.5$ would result in $R = 0.03\pm 0.04$, consistent with the upper limit we derived. Also the results of Mattson & Weaver and of Reeves et al. (2007) fit well on this correlation. The measurement of Molina et al. (2006) based on non-simultaneous *BeppoSAX* and *INTEGRAL* IBIS/ISGRI data however, with $R = 1.2$ and $\Gamma = 1.7$ lies about 7σ off this relation which results in $R = 0.13\pm 0.16$. This might indicate that it is indeed essential to study simultaneous observations when determining the strength of the reflection component.

3. Accretion power in MCG–05–23–016

MCG–05–23–016 presents a rather unique case. Its spectrum is, at least to the first order, nearly constant in shape and luminosity, with a possibly variable reflection component ($R = 0\ldots 1$) and high-energy cut-off ($E_C = 50\ldots 120\,\mathrm{keV}$). The overall luminosity is low. Using the X-ray luminosity of $L_{2-200\,\mathrm{keV}} = 10^{44}\,\mathrm{erg\,s^{-1}}$ as a proxy for the bolometric luminosity, the small black hole mass of $2\times 10^{6}\,\mathrm{M_\odot}$ [8] leads to a large Eddington ratio of $L_{bol}/L_{Edd} \gtrsim 0.4$. As the UV/optical emission is at least of the same order as the X-ray one, it is more likely that the Eddington ratio is as high as $L_{bol}/L_{Edd} \gtrsim 0.8$. Considering the error on the mass determination, this translates in a range of $L_{bol}/L_{Edd} = 0.2-5$.

An independent way to determine the mass of a black hole is to study its temporal behaviour. Following [20], the detection of a break in the X-ray power spectral density (PSD) of an AGN would allow to estimate the black hole mass thanks to the relation $\log T_B = 2.1\log(M_{BH}\times 10^{-6} M_\odot^{-1}) - 0.98\log(L_{bol}\times 10^{-44}\,\mathrm{erg^{-1}\,s}) - 2.32$. Using the data collected by *RXTE*/PCA and *XMM-Newton*/PN between 1996 and 2005, we estimated the X-ray PSD and structure function (*RXTE* data only) of MCG–05–23–016. The structure function has the advantage of working in the time domain and therefore being less sensitive to alias and windowing problems than the Fourier analysis. The PSD was calculated for each observation longer than 10 ks (on 200 seconds binned light curves), and the PSDs obtained were averaged and binned in logarithmically spaced bins [17]. The final PSD is shown in Figure 1. At high frequencies and down to $\sim 5\times 10^{-4}\,\mathrm{Hz}$ (2 ks) the PSD shows a flattening indicating the Poisson noise level of the light curves used. Then it increases towards lower frequencies and flattens again between $2\times 10^{-5} - 10^{-4}\,\mathrm{Hz}$ (10–50 ks), close to the minimum frequencies sampled by these data ($\sim 7\times 10^{-6}\,\mathrm{Hz}$). Also the structure function, shown in Figure 2, presents the hint of a break, but rather at $\sim$3.5 ks. The lack of a longer-term monitoring prevents us from drawing a firm conclusion about the presence and the position of the break. Assuming a break in the range 0.04–0.6 days (3.5–50 ks), we achieve a black hole mass of $M_{BH} = 0.4 - 1.4\times 10^{7}\,\mathrm{M_\odot}$. This range indicates a larger black hole mass than $2\times 10^{6}\,\mathrm{M_\odot}$. Using the latter value, the break in

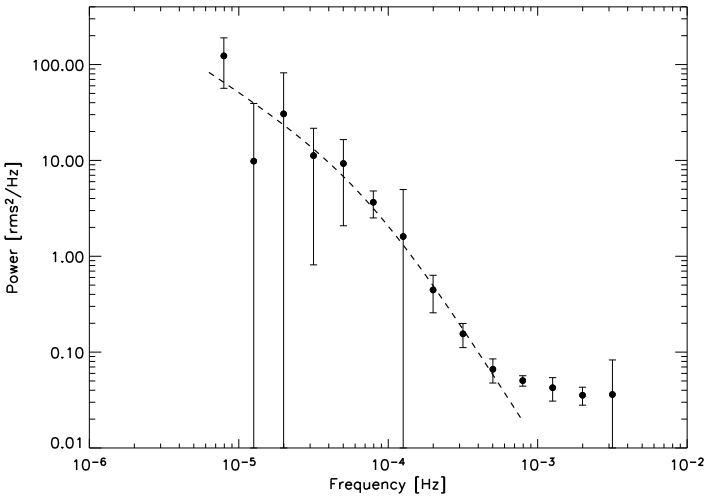

Figure 1: Power spectral density built using 9 *RXTE*/PCA plus 3 *XMM-Newton*/PN observations. All light curves were rebinned to 200 s and PCA data are in the 2–9 keV range, whereas the EPIC/PN ones are in the 0.2–12 keV band. The dashed line represents the fit to the data using the standard bending power law [18], with the low-frequency index fixed to -1. The fit results in a high-frequency index of -2.5 ± 0.5 and a break at 7×10^{-5} Hz.

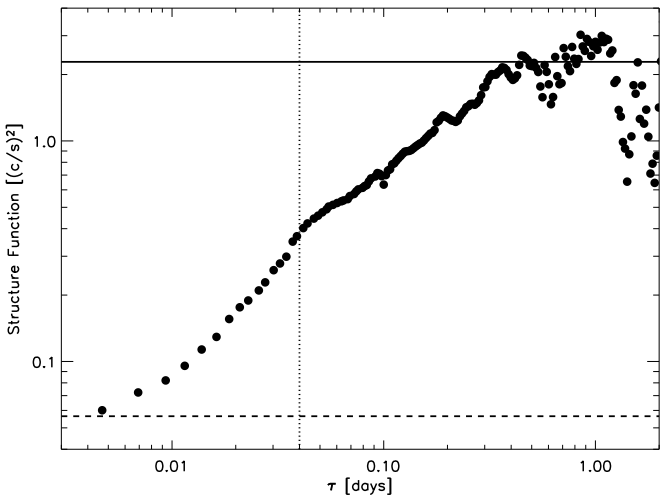

Figure 2: Structure function built with the full *RXTE*/PCA light curve (9 observations from 1996 to 2005), rebinned to 200s bins. The energy band used is 2–9 keV. The continuous and dashed lines indicate the values of the expected upper and lower plateaus, respectively. The vertical dotted line indicates the possible steepening time at 0.04 days (3.5 ksec), from a slope of 0.75 ± 0.09 on long time scales to 1.09 ± 0.03 at shorter time scales. The noise is dominating below 0.01 days (860 sec) and the flattening at 0.4 days (35 ks) corresponds to the average length of the single observations, therefore it does not indicate a maximum time scale of variability.

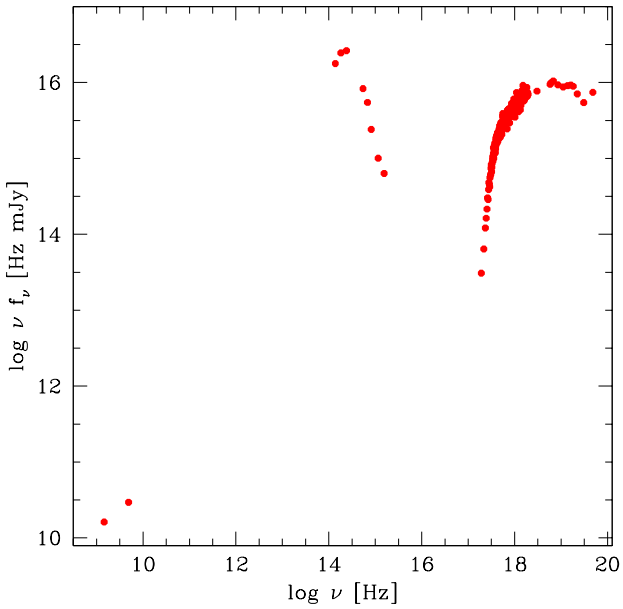

Figure 3: Spectral energy distribution of the combined data set, including *Swift*/UVOT optical and UV data as well as *Swift*/XRT soft X-ray, and *INTEGRAL* JEM-X and IBIS/ISGRI hard X-ray data. In addition, 2MASS measurements (J, H, and Ks) and radio data (6 cm and 20 cm) have been added. Data have been corrected for Galactic hydrogen column density, but not for intrinsic absorption.

the PDS would be expected to be around $T_B = 0.01\,\mathrm{days} = 0.9\,\mathrm{ksec}$. A break at this time would not be detectable in our data, as they are dominated by Poisson noise below 2 ksec.

Figure 3 shows the SED of the source for the data presented here, corrected for Galactic absorption of $N_{H,Gal} = 8 \times 10^{20}\,\mathrm{cm}^{-2}$ in the line of sight, giving an extinction of $A_V = N_\mathrm{H}/1.79 \times 10^{21}\,\mathrm{cm}^{-2} = 0.45\,\mathrm{mag}$. The extinction in the UV is higher (e.g. $A_U = 0.74\,\mathrm{mag}$), while the effect is insignificant in the near infrared with e.g. $A_K = 0.05\,\mathrm{mag}$. To the simultaneous data we added previous observations in the J, H, and Ks band from the 2MASS and VLA observations at 6 cm and 20 cm [21] for comparison. The SED indicates that the bolometric luminosity is probably $L_{bol} > 2L_X$. Even considering the uncertainty of the mass determination, the source cannot be assumed to be a typical low-luminosity AGN, which exhibits Eddington ratios in the range 10^{-3} to 10^{-6} [22], and the Seyfert 1.9 shows an Eddington ratio up to 10^8 times larger than that of Sgr A* which has a similar mass of $M = 3.3 \times 10^6\,\mathrm{M}_\odot$ [23]. If we assume that the mass is in fact $M \lesssim 5 \times 10^6\,\mathrm{M}_\odot$ then the Eddington ratio of $L_{bol}/L_{Edd} \gtrsim 0.8$ is also remarkable when compared to other Seyfert galaxies. Woo & Urry (2002) list a total of 32 Seyfert galaxies with black hole masses lower than $10^7\,\mathrm{M}_\odot$ and only 3 of them have $L_{bol}/L_{Edd} \gtrsim 1$, whereas the average of these lower mass black holes is $L_{bol}/L_{Edd} = 0.30 \pm 0.05$. In the Galactic equivalent, the hard state is usually reached at small Eddington ratios, like $L_{bol}/L_{Edd} \simeq 10^{-3}$ in the case of XTE J1118+480 [25], and $0.003 - 0.2$ for XTE J1550+564 [26]. In fact the SED of the X-ray nova XTE J1118+480 in the low state appears very similar to the one of MCG–05–23–016. In XTE J1118+480 the thermal disc component has a temperature as low as 24 eV. Considering that the temperature scales with $T \propto M^{-0.25}$, the disc emission of the Seyfert can be expected at much lower frequencies and

can be hidden in the SED component peaking around $10^{14.5}$ Hz. XTE J1118+480 also shows a power law component dominating the spectrum in the $0.4-160$ keV range with a photon index of $\Gamma = 1.8$ [27]. The overall SED in this object can be explained by an advection dominated accretion flow (ADAF) model at 2% Eddington ratio [25]. Although the SED of MCG–05–23–016 appears to resemble the one of XTE J1118+480, its high Eddington ratio is unlikely to be arising from a radiative inefficient accretion as described in the ADAF. An object with higher Eddington ratio also in the hard state is GX 339-4, which reaches $L_{bol}/L_{Edd} = 0.25$ in the hard state in some cases before the state transition into the high-soft state [28], consistent with MCG–05–23–016, although on average GX 339-4 reaches only an Eddington ratio of 0.015 and 0.05 during quiescence and during outburst, respectively. Considering a time scale for accretion rate changes in GX 339-4 of ~ 1000 days [28], this would correspond to time scales of ~ 1 Myr in the case of MCG–05–23–016, as the variation times scale with the mass of the black hole.

Objects which are thought to exhibit extremely high Eddington ratios are the ultra-luminous X-ray sources (ULX). The true nature of these objects is still unclear though. Considering their luminosity, they are either intermediate mass black holes (IMBH) with a central mass as high as $100-100,000\,M_\odot$, or alternatively they are operating at very high Eddington ratio, as large as $L_{bol}/L_{Edd} > 20$ [29]. ULX also show hard spectra and low temperature disc similar to XTE J1550–564 in very high state where the disc temperature decreases [30]. A study of *Chandra* data on ULX showed that the spectra can often be fitted by a simple power-law model, without evidence for thermal accretion disc components [31], similar to MCG–05–23–016. In some cases ULX show a disc component, e.g. the *XMM-Newton* observation of two ULX in NGC 1313 revealed soft components which are well fitted by multicolor disc blackbody models with color temperatures of $kT \simeq 150$ eV.

Low mass AGN like MCG–05–23–016 operating at high Eddington rate might be an early state in the evolution towards high-mass black holes as seen in quasars. As the highest measured redshift of a quasar to date is $z = 6.43$ [1], we can assume that these objects with black hole masses of $M > 10^8\,M_\odot$ appear in the Universe around $z \sim 7$. If we assume the formation of the first heavy black holes with $M \sim 10^6\,M_\odot$ at redshift $z = 10$, we indeed need high mass accretion rates. An object like MCG–05–23–016, if we consider its mass to be indeed $M \lesssim 5 \times 10^6\,M_\odot$, with a constant Eddington ratio of $L_{bol}/L_{Edd} = 0.8$ and starting black hole mass of $M(z=10) = 10^6\,M_\odot$ would reach a mass of $M(z=7) = 4 \times 10^8\,M_\odot$. However, this would require not only the existence of a super massive black hole with $M \sim 10^6\,M_\odot$ at redshift $z = 10$, but also a high accretion rate over a time span of 3×10^8 yrs. But even at a duty cycle of only 20% for AGN activity at $z \geq 7$, objects like MCG–05–23–016 can evolve to $10^8\,M_\odot$, and it has to be taken into account that the duty cycle of AGN is likely to be larger in the high-redshift Universe [32]. On the other hand, it has to be considered that the environment in which the AGN grows at redshifts $z > 7$ might be significantly different than the one we observe MCG–05–23–016 at in the local Universe.

References

[1] Willott, C. J., Delorme, P., Omont, A., et al. 2007, AJ, 134, 2435

[2] Kashlinsky, A., Arendt, R. G., Mather, J., & Moseley, S. H. 2005, Nature, 438, 45

[3] Gebhardt, K., Bender, R., Bower, G., et al. 2000, ApJ, 539, L13

[4] Uttley, P. & McHardy, I. M. 2004, PThPS, 155, 170

[5] Balestra, I., Bianchi, S., & Matt, G. 2004, A&A, 415, 437

[6] Soldi, S., Beckmann, V., Bassani, L., et al. 2005, A&A, 444, 431

[7] Beckmann, V., Barthelmy, S. D., Courvoisier, T. J.-L., et al. 2007, A&A, 475, 827

[8] Wang, J.-M., & Zhang, E. P. 2007, ApJ, 660, 1072

[9] Greene, J. E., & Ho, L. C. 2005, ApJ, 627, 721

[10] Tremaine, S., Gebhardt, K., Bender, R., et al. 2002, ApJ, 574, 740

[11] Reeves, J. N., Awaki, H., Dewangan, G. C., et al. 2007, PASJ, 59, 301

[12] Braito, V., Reeves, J. N., Dewangan, G. C., et al. 2007, ApJ, 670, 978

[13] Beckmann, V., Courvoisier, T. J.-L., Gehrels, N., et al. 2008, A&A, 492, 93

[14] Titarchuk, L. 1994, ApJ, 434, 570

[15] Molina, M., Malizia, A., Bassani, L., et al. 2006, MNRAS, 371, 821

[16] Mattson, B. J., & Weaver, K. A. 2004, ApJ, 601, 771

[17] Uttley, P., McHardy, I. M., & Papadakis, I. E. 2002, MNRAS 332, 231

[18] Uttley, P. & McHardy, I. M. 2005, MNRAS, 363, 586

[19] Zdziarski, A. A., Lubiński, P., & Smith, D. A. 1999, MNRAS, 303, L11

[20] McHardy, I. M., Koerding, E., Knigge, C., Uttley, P., & Fender, R. P. 2006, Nature, 444, 730

[21] Ulvestad, J. S. & Wilson, A. S. 1984, ApJ, 285, 439

[22] Ho, L. C. 1999, ApJ, 516, 672

[23] Schödel, R., Ott, T., Genzel, R., et al. 2002, ApJ, 596, 1015

[24] Woo, J.-H. & Urry, C. M. 2002, ApJ, 579, 530

[25] Esin, A. A., McClintock, J. E., Drake, J. J., et al. 2001, ApJ, 555, 483

[26] Done, C., & Gierliński, M. 2006, MNRAS, 367, 659

[27] McClintock, J. E., Haswell, C. A., Garcia, M. R., et al. 2001, ApJ, 555, 447

[28] Zdziarski, A. A., Gierliński, M., Mikołajewska, J., et al. 2004, MNRAS, 351, 791

[29] Soria, R., Baldi, A., Risaliti, G., et al. 2007, MNRAS, 379, 1313

[30] Kubota, A., & Done, C. 2004, MNRAS, 353, 980

[31] Berghea, C. T., Weaver, K. A., Colbert, E. J. M., & Roberts, T. P. 2008, ApJ, 687, 471

[32] Wang, J.-M., Chen, Y.-M., Yan, C.-S., & Hu, C. 2008, ApJ, 673, L9